Available online at www.sciencedirect.com
ScienceDirect
Catalysis Today 124 (2007) 124–132
CATALYSIS TODAY
www.elsevier.com/locate/cattod

Photocatalytic oxidation of multicomponent systems of herbicides: Scale-up of laboratory kinetics rate data to plant scale

Gianluca Li Puma *, Bea Toepfer, Alexander Gora

Photocatalysis & Photoreaction Engineering, School of Chemical, Environmental and Mining Engineering, The University of Nottingham, University Park, Nottingham NG7 2RD, United Kingdom

Available online 7 May 2007

Abstract

The reaction kinetics of the photocatalytic oxidation (PCO) of the herbicides isoproturon, simazine and propazine over irradiated TiO_2 (Degussa P25) suspensions were studied in multicomponent systems in a laboratory-scale annular photoreactor operated in recirculation batch mode. The multicomponent kinetic model established was then extended to take into account the direct effect of radiation absorbed by the TiO_2 photocatalyst in order to obtain intrinsic kinetic parameters independent of the radiation field in the photoreactor. An analysis of the radiation field in the photoreaction space was accomplished using a recently published Six-Flux Radiation Absorption-Scattering model (SFM) to decouple the values of the apparent reaction kinetic constants from the local volumetric rate of photon absorption (LVRPA) in the rate law of PCO of herbicide. The resulting rate laws with explicit dependence on the LVRPA were then used to predict, through accurate reactor modeling, the degradation of the herbicides in an optimal configuration of a flow-through, pilot-scale, falling film photoreactor. In a plant treatment scenario the total operating costs of the PCO of herbicides were calculated to be 3.75 Euro m^{-3}.

Keywords: Water purification; Titanium dioxide; Photocatalysis; Pesticides; Suspensions; Langmuir–Hinshelwood; Falling film; Pilot plant

1. Introduction

Herbicides are widely used in agriculture to control weed growth in crops. As a result, their residues are found in rivers, lakes, underground waters and drinking water supplies [1–4]. The elimination of herbicides in drinking water usually involves the use of granular activated carbon, however, this treatment process tends to be inefficient at the lowest concentration levels (ppb or ppt) and with polar compounds and ultimately does not eliminate the herbicides from the environment. Photocatalytic oxidation (PCO) provides a feasible route for the destruction of trace concentrations of herbicides from the environment and in drinking water [5–7].

PCO occurs as a result of the interaction of a semiconductor photocatalyst and UV radiation that yields highly reactive hydroxyl radicals, which are believed to be the main species responsible for the oxidation of organic substrates [8]. The most commonly used photocatalyst is titanium dioxide (TiO_2), which is inexpensive, abundant, photostable and non-toxic.

PCO kinetics of many organic substrates have been analyzed in terms of pseudo Langmuir–Hinshelwood (L–H) rate equations. However, the fitting of experimental data with L–H type kinetic models has so far only been demonstrated for the PCO of organic substrates in single-component systems [5,8–10]. In general, kinetic studies of the PCO of multi-component systems composed of different organic substrates, which compete for the active sites on the surface of the photocatalyst, can rarely be found in the literature. Furthermore, pseudo L–H kinetic parameters are usually determined without the explicit consideration of photon absorption and scattering in the reactor, unless an accurate analysis of the radiation field in the photoreactor has been implemented in the kinetic model. As a result, the rate laws and kinetic parameters are not scalable to reactors of different size or geometry and the resulting L–H type kinetic model remains a property of the reactor from which it was derived. This is probably the reason why most pilot-scale photoreactors are still designed using empirical (build and test) or semi-empirical methods.

* Corresponding author. Tel.: +44 115 951 4170; fax: +44 115 951 4115.
E-mail address: gianluca.li.puma@nottingham.ac.uk (G. Li Puma).

0920-5861/$ – see front matter © 2007 Elsevier B.V. All rights reserved.
doi:10.1016/j.cattod.2007.03.047

Nomenclature

a	model parameter SFM
A	geometrical coefficient
b	model parameter SFM
c_{cat}	photocatalyst concentration (kg m^{-3})
C	substrate concentration (mol m^{-3})
C_0	herbicide concentration at initial time or in the feed stream to reactor (mol m^{-3})
C_N	herbicide concentration at the exit of N reactors in series (mol m^{-3})
H	length of the reactor (m)
I	radiation intensity (or radiative flux) (W m^{-2})
I_λ	radiation intensity divided wavelength of radiation (W m^{-3} nm^{-1})
$I^{max}_{\xi=0}$	maximum value of radiation intensity at surface $\xi = 0$ (W m^{-2})
$I^*_{\xi^*,z^*}$	dimensionless radiation intensity or dimensionless LVRPA ($=I_{\xi,z}/I^{max}_{\xi=0}$)
k	kinetic constant (mol m^{-3} s^{-1})
k_T	kinetic constant independent of radiation absorbed (mol s^{-1} m^{-3} (W m^{-3})$^{-0.5}$)
K	binding constant (m^3 mol^{-1})
L	lamp length (m)
(LVRPA)	local volumetric rate of photon absorption (W m^{-3})
$(LVRPA)^*$	dimensionless local volumetric rate of photon absorption ($=(LVRPA)/(LVRPA)^{max}_{\xi^*=0}$)
m	order of the reaction with respect to the LVRPA
N_{Da}	Damköhler number
N_{Re}	Reynolds number
n	number of herbicides in solution
N	number of reactors in series
p_b	probability of photon scattering in the backward direction
p_f	probability of photon scattering in the forward direction
p_s	probability of photon scattering in the side direction
Q^0	volumetric flow rate fed to reactor module (m^3 s^{-1})
Q^R	volumetric flow rate of falling film down the column (m^3 s^{-1})
r	radial coordinate (m)
r^*	dimensionless radial coordinate ($=r/R$)
r_j	rate of the reaction with respect to herbicide j (mol s^{-1} m^{-3})
r_l	lamp radius (m)
R	external radius of annulus (m)
t	time (s)
X	single pass conversion
X_{series}	overall conversion in N reactor in series
v	fluid velocity (m s^{-1})
V	total volume of fluid in recirculation system (the reactor, the tubing, the feed tank) (m^3)
V_r	reactor volume (the physical space occupied by the liquid in the reactor) (m^3)
z	axial coordinate (m)
z^*	dimensionless axial coordinate ($=z/H$)

Greek letters

α	geometrical parameter ($=H/L$)
β	geometrical parameter ($=L/\eta R$)
γ	dimensionless parameter SFM
δ	thickness of the annulus or of the falling film (m)
η	ratio of internal radius to external radius of annulus
κ	specific mass absorption coefficient averaged over the spectrum of the incident radiation (m^2 kg^{-1})
λ	radiation wavelength (m)
ν	kinematic viscosity (m^2 s^{-1})
ξ	reaction space radial coordinate or film thickness coordinate (m)
ξ^*	dimensionless reaction space radial coordinate or film thickness coordinate ($=\xi/\delta$)
σ	specific mass scattering coefficient averaged over the spectrum of the incident radiation (m^2 kg^{-1})
τ	optical thickness
τ_{app}	apparent optical thickness
χ_j	conversion of j in reactor with recycle
ψ	recycle ratio
ω	scattering albedo ($=\sigma/(\sigma+\kappa)$)
ω_{corr}	corrected scattering albedo SFM

Subscripts

i	intermediate reaction product
j	herbicide
l	lamp
max	maximum
min	minimum
λ	wavelength
ηR	position at inner wall of annulus
w	lamp wall
z, z^*	direction along the axial coordinate
ξ, ξ^*	direction along the film transversal coordinate
0	position at inner wall of annulus

Superscripts

*	dimensionless variable
in	position at inlet of the reactor
max	maximum value
out	position at outlet of the reactor

In this study we rationalize these aspects and we begin by describing the results of an accurate kinetic study of the photocatalytic oxidation of multicomponent systems of three of the most common herbicides: isoproturon, simazine and propazine (Fig. 1). This study, carried out in laboratory-scale annular photoreactor operated in a recirculation batch mode, yielded kinetic parameters that are independent of the radiation field in the photoreactor. We then consider an optimal

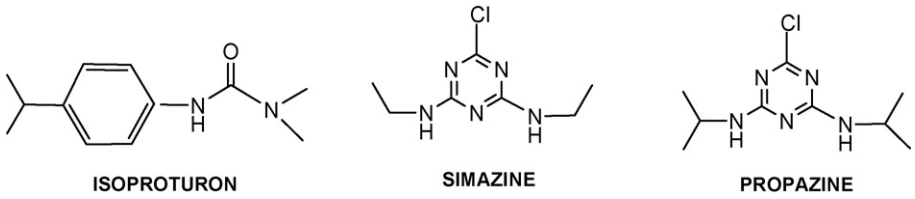

Fig. 1. Molecular structure of the herbicides studied.

configuration of a pilot-scale, continuous flow ''falling film'' reactor utilizing a single, commercially available, UVA lamp. In this paper, we describe the modeling of the reactor and the scale-up of the herbicide treatment process to predict by numerical simulations the herbicide conversions. Finally, we estimate the operating cost for a plant-scale PCO reactor network.

2. Methods

2.1. Laboratory-scale annular photoreactor

Materials, methods, equipment and analytical procedures were the same as those reported previously [11,12]. Briefly, photocatalytic experiments on the herbicides (Pestanal, Analytical Standard, >99%, Riedel-de Haën) were carried out in a 0.134 L annular photocatalytic reactor irradiated with an eight Watt UVA lamp (Philips TL 8W/08 F8 T5/BLB). The reactor is described in detail elsewhere [11,12]. The reactor was operated in a recirculation batch mode (Fig. 2) with 0.4 g L^{-1} of a suspension of TiO_2 (Degussa P25) in ultrapure water. The total volume of the suspension in the system was 2 L. Samples collected at appropriate time intervals were filtered through 0.45 μm, 25 mm EasyDisc nylon filters (Whatman) to remove the TiO_2 particles and promptly analyzed by an Agilent 1100 series high performance liquid chromatograph system fitted with a diode array detector and autosampler. The initial concentration of each herbicide was in the range 3 mg L^{-1} to 70 μg L^{-1} and the reaction were followed down to the HPLC

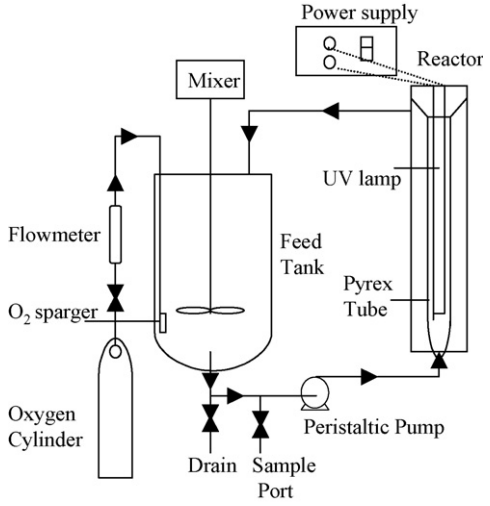

Fig. 2. Schematic diagram of the laboratory-scale, annular photocatalytic reactor system.

detection limit (0.16 μg L^{-1} for isoproturon, 3.2 μg L^{-1} for simazine, and 7.2 μg L^{-1} for propazine). Experiments at different photon fluxes were carried out by changing the power supplied to the lamp using a variable power supply unit. The UV-A photon flux at the lamp wall, in the wavelength interval between 343 nm and 380 nm, was varied in the range from 36.5 W m^{-2} to 67.1 W m^{-2} [12].

3. Results and discussion

3.1. Multicomponent herbicide degradation kinetics

In our previous study [11] isoproturon was found to degrade at a much faster rate (approximately four times higher) than simazine and propazine. This was explained by a higher degree of photocatalyst surface coverage of isoproturon as shown by the dark adsorption studies and by the accessibility of its molecular structure to OH radical attack. In contrast, simazine and propazine exhibited similar rates of degradation, as anticipated considering the similarity of the molecular structures. Moreover, simazine and propazine yield cianuric acid as the final oxidation product, while isoproturon can be fully mineralized to CO_2 and organic acids. In multicomponent experiments with equimolar solutions of all three herbicides, they were found to degrade at lower rates than when analyzed in single-component experiments suggesting competitive inhibition kinetics among the herbicides. This competition was modeled by the L–H rate laws [11] as shown below:

$$-r_j = \frac{k_j K_j C_j}{1 + \sum_{j=1}^{n} K_j C_{0j}} \qquad \text{with } j = 1, 2, \ldots, n \tag{1}$$

where k_j (mol L^{-1} s^{-1}) and K_j (L mol^{-1}) are the reaction kinetic constant and binding constant of the herbicide j respectively, C_j (L mol^{-1}) is the concentration of herbicide in solution, C_{0j} (L mol^{-1}) the concentration of herbicide in solution at the initial time (batch reactor) or in the reactor feed (flow-through reactor) and n is the number of herbicides in solution.

Note that the denominator in Eq. (1) takes into account the effect of the intermediate reaction products since it assumes a stepwise reaction scheme with identical binding constants of the intermediates and the herbicide such that:

$$K_j C_j + \left(\sum K_i C_i \right)_j = K_j C_{0j} \tag{2}$$

where K_i (L mol^{-1}) is the binding constant of the intermediate product adsorbed onto the surface of TiO_2 and C_i is the concentration of the intermediate in solution.

Table 1
Herbicide binding constants on TiO_2 Degussa P25 measured in the dark and under UVA irradiation at natural pH of the suspension ($C_{0j} \leq 1$ mg L^{-1}) [11]

Herbicide	$K_{dark} \times 10^5$ (L mol^{-1})	$K_{UV} \times 10^5$ (L mol^{-1})
Isoproturon	6.2087 ± 0.739	5.7926 ± 0.6012
Simazine	3.4982 ± 0.143	6.1005 ± 0.9654
Propazine	3.0435 ± 0.262	4.2802 ± 0.7899

The kinetics parameters k_j (mol L^{-1} s^{-1}) and K_j (L mol^{-1}) were determined from single-component experiments with each herbicide and they where substituted in Eq. (1) to model the time-dependent degradation profiles of multicomponent systems of herbicide. The results presented in Gora et al. [11] show that a reasonably good fit of the degradation profiles of multicomponent herbicides mixtures was obtained when using the kinetic approximation of Eq. (2). When the reaction intermediates were ignored in the kinetic model (replace C_{0j} with C_j in Eq. (1)) an overestimation of the degradation was observed for the experiments conducted at the initial herbicide concentrations approaching monolayer saturation of the TiO_2 surface. Thus, it was concluded that the reaction intermediates do play an important role in determining the degradation kinetics of the herbicides and that these must be taken into account in the kinetic rate laws (Eq. (1)).

The L–H rate equations were successfully extended to represent the time-dependent degradation profiles of multicomponent systems of herbicides, using the kinetic parameters determined in single-component experiments. Contrary to previous published work [10] the binding constants of the herbicides observed under dark adsorption and under PCO were found to be of the same order of magnitude (Table 1) therefore it was suggested that the degradation of isoproturon, simazine and propazine and their mixtures follow a surface or near-surface reaction according to a competitive L–H mechanism. The above findings were observed only at herbicide concentrations less than approximately 1 mg L^{-1} at which monolayer coverage of TiO_2 is attained. Above 1 mg L^{-1} it was concluded that there is a departure from the L–H mechanism due to multilayer adsorption of the herbicides leading to faster herbicide degradation kinetics.

3.2. Herbicide reaction kinetics with explicit photon absorption effects

In general, PCO reaction kinetics equations presented in the literature are applicable to the photoreactor geometry and the experimental conditions under which they have been established, unless an analysis of the radiation field in the photoreactor has been implemented in the kinetic model. Various forms of these rate laws presented in the literature show Langmuirian dependence on the substrate concentration and either power law dependence on the incident photon flux at the front wall of the photoreactor, or power law dependence on the overall radiation absorbed in the photoreactor. The dependence of the apparent reaction kinetic constants on the radiation absorbed within the photoreactor must be established if the kinetic model is to be made scalable to photoreactors of any size or geometry. To accomplish this task, the radiation field in the photoreactor must be modeled, which involves solving the radiative transfer equation (RTE) for the participating media [13]. This yields the spatial distribution of the local volumetric rate of photon absorption (LVRPA) which must appear in the kinetic rate law of the substrates [14].

Dark adsorption studies of the herbicides ($C_{0j} \leq 1$ mg L^{-1}) over the photocatalyst (TiO_2 Degussa P25) revealed that the values of the binding constants were of the same order of magnitude as those measured under UV irradiation, (Table 1). In consequence, it may be reasonably concluded that the K_j values in Eq. (1) are independent of radiation absorption. The L–H kinetic constant k_j therefore is the only kinetic parameter which might depend on the LVRPA within the reaction space. In accordance with mechanistic studies of PCO of organic substrates in the literature [15-16], a power law dependence of the reaction rate constant on the LVRPA may be suggested to model the PCO kinetics of multicomponent herbicides as shown below:

$$-r_j = k_{T,j}(\mathrm{LVRPA})^m \frac{K_j C_j}{1 + \sum_{j=1}^{n} K_j C_{0j}} \quad (3)$$

In Eq. (3) above $k_{T,j}$ is a kinetic constant independent of photon absorption and including the primary quantum yield for electron-hole generation within the photocatalyst, LVRPA is the local volumetric rate of photon absorption. Eq. (3) is strictly valid for monochromatic irradiation only. In the case of polychromatic radiation the LVRPA may be averaged over the useful spectrum of the incident radiation up to wavelengths less than 380 nm for TiO_2 Degussa P25 [12]. However, caution should be exercised in this case, especially when using lamps with irregular emission spectrums, as using the averaged LVRPA is clearly not rigorous and may lead to errors. The exponent m of the LVRPA depends on the efficiency of electron–hole formation and recombination at the catalyst surface and takes a value between 0.5 and 1 providing the reaction is kinetically controlled. Kinetic studies on the effect of the incident radiation have shown that at weak intensities the observed rate of oxidation is first-order with respect to radiation intensity [17], and shifts to half-order once the rate of electron-hole formation becomes greater than the photocatalytic rate, favouring electron–hole recombination [18].

The analysis of the radiation field in the photoreaction space was accomplished using the Six-Flux Radiation Absorption-Scattering model (SFM) [12,19–21] to decouple the values of the apparent reaction kinetic constants from the LVRPA in the rate law of herbicide PCO. The SFM assumes that photon scattering fluxes can occur along the six directions of the Cartesian coordinates only. The SFM yields a realistic representation of the LVRPA in the reaction space, with computational time needs in the range of a few minutes on a standard PC.

The optical parameters of the TiO_2 suspension necessary to evaluate the LVRPA using the SFM were determined under the prevalent condition of particle agglomeration in the reactor [12] and are reported in Table 2.

Table 2
Optical parameters of the TiO_2 (Degussa P25) suspension averaged over the wavelength range 343 nm to 380 nm [12]

Model parameter	Value
Scattering albedo, ω	0.8617
Specific absorption coefficient	186.7 $m^2\,kg^{-1}$
Specific scattering coefficient	1163.3 $m^2\,kg^{-1}$

The LVRPA at each point in the reaction space of the annular photoreactor calculated with the SFM is:

$$\mathrm{LVRPA} = \frac{\tau_{\mathrm{app}} I_0}{\omega_{\mathrm{corr}}(1-\gamma)(1-\eta)R} \times \frac{\eta}{[\eta+(1-\eta)\xi^*]}[(\omega_{\mathrm{corr}}-1 + \sqrt{1-\omega_{\mathrm{corr}}^2})\exp(-\tau_{\mathrm{app}}\xi^*) + \gamma(\omega_{\mathrm{corr}}-1-\sqrt{1-\omega_{\mathrm{corr}}^2})\exp(\tau_{\mathrm{app}}\xi^*)] \quad (4)$$

The apparent optical thickness τ_{app} of the reaction space is related to the "characteristic extinction length" of photons when radiation scattering is present and corresponds to the optical thickness, which would be measured using a "geometrically thick" photoreactor system with scattering particles. In the derivation of Eq. (4) negligible absorption of radiation by the fluid and by the dissolved species was assumed compared to the absorption of radiation by the photocatalytic particles. As a result, the LVRPA is independent of time. This assumption is most often valid with diluted solutions of weakly absorbing species, such as herbicides. Further assumptions invoked in the derivation of Eq. (4) are reported in Toepfer et al. [12] (note that Eq. (4) in reference [12] is missing a term at the denominator due to a typographical error). Further details on the SFM and its complete derivation from first principles have been reported in other papers [19–21].

The rate law (Eq. (3)) was combined with the LVRPA (Eq. (4)) and with the material balance in the batch recirculation reaction system, which has total volume (V) and reactor volume (V_r). It was integrated using the initial conditions ($t = 0$, $C_j = C_{0j}$ with $j = 1, 2, \ldots, n$) to yield the time-dependent degradation profiles of each herbicide in a multicomponent experiment [12]:

$$C_j = C_{0j}\exp\left(-\frac{K_j}{V}\frac{k_{\mathrm{T},j}\left(\int_{V_r}(\mathrm{LVRPA})^m\,\mathrm{d}V_r\right)}{1+\sum_{j=1}^{n}K_jC_{0j}}\times t\right) \quad (5)$$

where n is the number of herbicides in solution. Note that V_r is the physical space occupied by the liquid in the reactor and V is total volume of fluid in the recirculation system comprising the reactor, the tubing and the feed tank.

3.3. Herbicide kinetic parameters

One of the main objectives of this work was to demonstrate fitting of the degradation profiles of multicomponent solutions of herbicides using kinetic constants determined from single-component experiments. The kinetic parameters in Eqs. (3) and (5) where determined using a linearized plot method from single-herbicide experiments ($n = 1$) as reported in Toepfer et al. [12] and the values which apply to the photocatalytic oxidation of isoproturon, simazine and propazine are reproduced in Table 3. The parameter m in Eq. (3) and (5) was determined to be 0.5 (photocatalyst electron–hole recombination prevails) under the range of photon fluxes investigated [12].

Table 3
Intrinsic kinetic parameters independent of radiation absorption [12]

Herbicide	Kinetic parameters	
	$k_{\mathrm{T},j}\times 10^{-6}$ (mol L^{-1} min^{-1} × (W m^{-3}) $^{-0.5}$)	$K_j \times 10^5$ (L mol^{-1})
Isoproturon	35.751 ± 0.291	5.7926 ± 0.6012
Simazine	9.6674 ± 0.077	6.1005 ± 0.9654
Propazine	10.831 ± 0.062	4.2802 ± 0.7899

Eq. (5) with the kinetic parameters shown in Table 3 was found to provide a satisfactory fit of the degradation profiles of isoproturon, simazine and propazine in equimolar and non-equimolar multicomponent experiments proving the validity of the model [12]. It is important to recognize that this model should be used only when the overall initial herbicide concentration is less than approximately 1 mg L^{-1}.

3.4. Herbicide conversions in a pilot-scale falling-film photoreactor

3.4.1. Pilot-scale falling film photoreactor

The reactor design of a pilot-scale falling film photoreactor (Fig. 3) has been described in previous papers [22,23]. The reactor geometry is specifically designed for optimal absorption of radiation emitted by a single, commercially available UVA lamp. It consists of a vertical stainless steel hollow column in which a falling film of a slurry suspension of TiO_2 flows along the internal wall of the column. A 36 W UVA blacklight lamp (Philips TL-D 36W/08 SLV) is suspended in the centre of the column and protected by a borosilicate glass lamp shield. Since the falling film has a free surface and does not touch the lamp

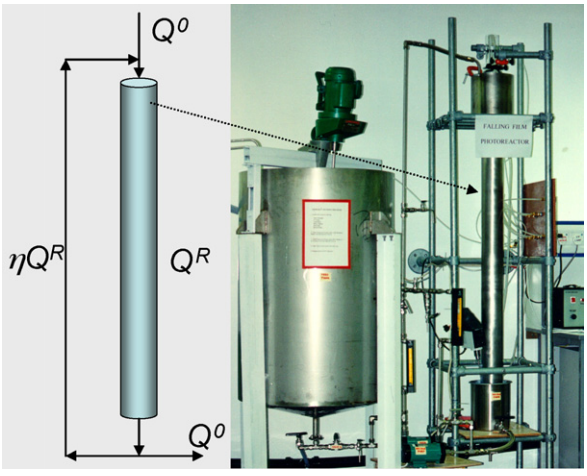

Fig. 3. Schematic diagram of pilot-scale, falling-film photoreactor.

Table 4
Specifications of pilot-scale falling film photoreactor and operating conditions.

Photoreactor dimensions	
Length, H	1.6 m
Inner radius, L	0.108 m
Lamp specifications	
Lamp type	Philips TL-D 36W/08 SLV
Nominal power rating	36 W
Bulb length, L	1.2 m
Bulb radius, r_1	0.014 m
Lifetime	12000 h
Photon flux at lamp wall, $\int_{343\,nm}^{380\,nm} I_{w,\lambda}\,d\lambda$	44.2 W m^{-2}
Geometrical parameters	$\alpha = 1.333$; $\beta = 22.222$
Falling film fluid-dynamics	
Flowrate down the column ($Q^0 + Q^R$)	40.4 L min^{-1}
Film thickness, δ	0.481×10^{-3} m
Film Reynolds number	725 (laminar)
Optical parameters (TiO_2 Degussa P25)	As in Table 2

shield, the incident photon flux reaching the thin-film suspension remains constant over time. This is not the case in conventional annular photoreactors which are affected by the problem of ''filming'' of the inner wall of the annulus.

The radiation emission spectra of the UV lamps used in the pilot- and laboratory-scale reactors are identical [12,24] although the power rating and lamp dimensions are different. The simulation results presented in this study pertain to operating the reactor at steady-state in a continuous flow mode with a partial recycle, i.e., a fraction of the product stream is recirculated back to the inlet of the reactor. The falling film reactor is operated under laminar flow conditions to provide optimal correspondence between fluid residence time and radiation field [25] while maintaining a high processing rate and optimum catalyst loading. Table 4 presents the specifications of the pilot-scale falling film photoreactor and operating conditions.

3.4.2. Modeling of falling-film photoreactor

The conversion expected in the pilot-scale falling film photoreactor can be predicted by a mathematical model of the photoreactor which analyzes appropriately radiation emission from the lamp, radiation absorption and scattering in the reaction space and the fluid dynamics. Like every model, a number of assumptions must be made and these should be judged to obtain the optimal trade-off between accuracy of the

Table 5
Mathematical model of the pilot-scale falling-film photocatalytic reactor[a]

Geometry of falling film	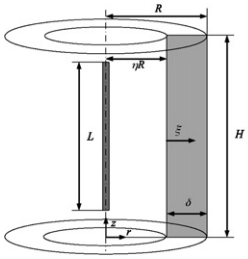 Dimensionless Design Parameters $\alpha = \frac{H}{L};\ \beta = \frac{L}{\eta R}$ Falling-film annular geometry ($\eta \approx 1$)
Dimensionless variables	$\xi^* = \frac{\xi}{\delta};\ r^* = \frac{r}{R};\ z^* = \frac{z}{H};\ v_z^* = \frac{v_z}{v_z^{max}};\ C_j^* = \frac{C_j}{C_j^{in}};\ (\mathrm{LVRPA})^* = \frac{(\mathrm{LVRPA})}{(\mathrm{LVRPA})_{\xi^*=0}^{max}} = I_{\xi^*,z^*}^* = \frac{I_{\xi,z}}{I_{\xi=0}^{max}}$
Velocity profile and Reynolds number	$(N_{Re} < 750)$: $v_x^* = 1 - \xi^{*2}$; $v_z^{max} = \frac{3}{2} v_{z,aerage}$; $N_{Re} = \frac{2R(1-\eta)v_z^{average}}{\nu} = \frac{2\delta v_z^{average}}{\nu}$
Scattering albedo and optical thickness	$\omega = \frac{\sigma}{\sigma+\kappa}$; $\tau = (\sigma+\kappa)c_{cat}\delta$
Maximum radiation intensity at surface ($\xi^* = 0$)	$I_{\xi^*=0}^{max} = f(\omega,\tau)\frac{r_l}{\eta R}\arctan\left(\frac{\beta}{2}\right)\int_{\lambda_{min}}^{\lambda_{max}} I_{w,\lambda}\,d\lambda$
Maximum LVRPA at surface ($\xi^* = 0$)	$(\mathrm{LVRPA})_{\xi^*=0}^{max} = \kappa c_{cat} I_{\xi^*=0}^{max} = (1-\omega)\frac{\tau}{\delta} I_{\xi^*=0}^{max} = (1-\omega)\frac{\tau}{R(1-\eta)} I_{\xi^*=0}^{max}$
Dimensionless radiation intensity at inner wall ($\xi^* = 0$)	$I_{\xi^*=0,z^*}^* = \frac{\arctan[\beta/2(2\alpha z^* - \alpha + 1)] - \arctan[\beta/2(2\alpha z^* - \alpha - 1)]}{2\arctan(\beta/2)}$
Dimensionless LVRPA and radiation model parameters	Six-flux absorption-scattering model ($\eta = 1$)
	$(\mathrm{LVRPA})^* = I_{\xi^*=0,z^*}^* \exp(-\tau_{app}\xi^*)$
	$f(\omega,\tau) = \left(1 + \frac{1}{\omega_{corr}}\left(1 - \frac{1+\gamma}{1-\gamma}\sqrt{1-\omega_{corr}^2}\right)\right)\left(1 + \frac{4\omega p_s}{1-\omega p_f - \omega p_b - 2\omega p_s}\right)$
	$a = 1 - \omega p_f - \frac{4\omega^2 p_s^2}{(1-\omega p_f - \omega p_b - 2\omega p_s)}$; $b = \omega p_b + \frac{4\omega^2 p_s^2}{(1-\omega p_f - \omega p_b - 2\omega p_s)}$
	$\omega_{corr} = \frac{b}{a}$; $\gamma = \frac{1-\sqrt{1-\omega_{corr}^2}}{1+\sqrt{1-\omega_{corr}^2}}\exp(-2\tau_{app})$; $\tau_{app} = a\tau\sqrt{1-\omega_{corr}^2}$
Herbicides rate equation	$-r_j = k_{T,j}(\mathrm{LVRPA})^{0.5}\frac{K_j C_j}{1+\sum_{j=1}^{n} K_j C_{0j}}$ $j = 1,2\ldots,n$ = number of herbicides in solution.
Material balance and Damköhler number	$v_z^* \frac{dC_j^*}{dz^*} = -N_{Da}(\mathrm{LVRPA}^*)^{0.5}(C_j^*)$; $N_{Da} = \frac{k_{T,j}K_j}{1+\sum_{j=1}^{n} K_j C_{0j}} \frac{(\mathrm{LVRPA}_{\xi^*=0}^{max})^{0.5} H}{v_z^{max}}$
Transversal distribution of herbicide j at reactor outlet and conversion	$C_{j,\xi^*}^{*out} = \exp\left[1 - A\frac{N_{Da}\exp(-m\tau_{app}\xi^*)}{v_z^*}\right]$; $A = \int_0^1 (I_{\xi^*=0,z^*}^*)^m\,dz^*$; $\gamma_j = 1 - \frac{v_z^{max}}{v_z^{average}}\int_0^1 v_z^* C_{j,\xi^*}^{*out}\,d\xi^*$
Conversion of j in reactor with recycle	$\chi_j = \frac{\gamma_j}{1-\eta(1-\gamma_j)}$, $\eta = \frac{Q^R - Q^0}{Q^0}$.

Adapted from [20,25], implementing the SFM [19–21] and herbicide kinetics from [12].

[a] Assumptions: (i) negligible air friction, (ii) inviscid fluid, (iii) constant surface tension, ξ, (iv) steady-state falling film laminar flow. Other assumptions see main text.

model predictions and complexity of the model. In our judgement the model reported in dimensionless form by Li Puma and Brucato [20] reaches the optimal trade-off for reactor design and optimization purposes. The model was previously experimentally verified for the photocatalytic oxidation of salicylic acid [25]. In Table 5 we present the complete model of the falling-film photoreactor with radiation absorption described by the six-flux absorption-scattering model under the assumption that the apparent optical thickness τ_{app} of the photoreactor is large enough to make γ a small number such that $(1-\gamma)\approx 1$. This is the case for an optically thick photoreactor, which corresponds to negligible radiation flux leaving from the outer wall of the annulus ($r = R$) as would be expected in optimized commercial photoreactors. In addition, the degradation kinetics of each herbicide is described by Eq. (3) with the parameter $m = 0.5$ and kinetic parameters from Table 3. The hydrodynamics of the falling film is represented by the laminar flow model which is applicable at Reynolds numbers less than 750 [26]. The emission of radiation from the lamp is modeled using the Linear Source Spherical Emission (LSSE) model [27]. The essential dimensionless model parameters necessary to calculate the conversion expected in the falling-film photoreactor are the apparent optical thickness τ_{app} described earlier, the Damkholer number, N_{Da}, (which in this case has the meaning of the ratio of the overall reaction rate, calculated at the inlet concentration and at the maximum photon flux, to the maximum input mass flow rate of the reactant) and the dimensionless design parameters of the reactor α and β.

3.4.3. Herbicide conversions in N pilot-scale reactors in series

The pilot-scale falling film photoreactor described above can be taken to be an optimized modular reactor system, thus, scale-up can be realized by connecting a number of the above reactors either in series or in parallel or in a combination of both. The effect of TiO_2 catalyst loading on herbicide conversions in one reactor module is shown in Fig. 4 for a selected feed flow rate (0.4 L min^{-1}). The conversions increase in the range from 0 to 6.5 kg m^{-3} as result of an increase in the absorption of radiation as the catalyst concentration is increased, however, above 6.5 kg m^{-1} the conversions decrease as a result of the reduction of the penetration depth of radiation through the suspension. In the case of the falling film laminar flow velocity profile considered here, the optimal TiO_2 concentration tends to shift towards higher catalyst concentrations compared to operation under the turbulent plug flow falling film velocity profile as a result of the effect of the advection transport through the z direction, which is more prominent at $\xi = 0$ [20]. From a practical point of view, the reactor network can be operated at a catalyst concentration of 3 kg m^{-3} (optical thickness $\tau = 1.94$; apparent optical thickness $\tau_{app} = 1.17$) which should maintain herbicide conversions close to maximum. As a result this value was selected for use in further simulations.

Since the herbicide rate laws are first-order in herbicide concentration, the Damkholer number is independent of

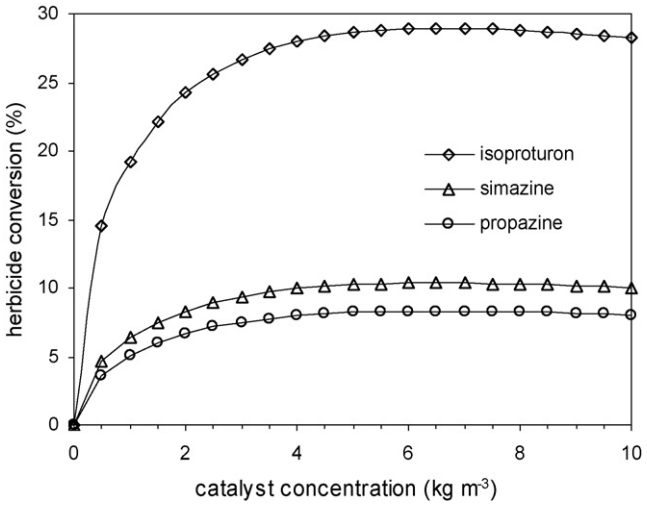

Fig. 4. Model simulations of the effect of TiO_2 catalyst loading on conversions of a multicomponent herbicide solution ($C_{0j} = 0.33$ mg L^{-1} each) in the pilot-scale falling film photoreactor. $Q^0 = 0.4$ L min^{-1}; diffuse photon scattering ($p_b = 0.71$; $p_f = 0.11$; $p_s = 0.045$) [21]; other experimental condition from Table 4.

herbicide concentration, as well as the herbicide conversions. Thus, for a fixed set of herbicide concentrations in the feed (C_{0j}) the overall conversion in N reactors in series is:

$$X_{series} = \frac{C_{0j} - C_{Nj}}{C_{0j}} = 1 - (1 - \chi_j)^N \quad (6)$$

where χ_j is the conversion in one reactor module as calculated from the model in Table 5.

Fig. 5 shows the herbicide conversions as a function of the number of reactor units connected in series for a feed flow rate of 0.4 L min^{-1} and herbicide concentrations in the feed of 0.33 mg L^{-1} each (upper limit of applicability of herbicide rate laws). Isoproturon is practically eliminated in 20 reactors, and the conversion of simazine and propazine is near 80%. By reducing

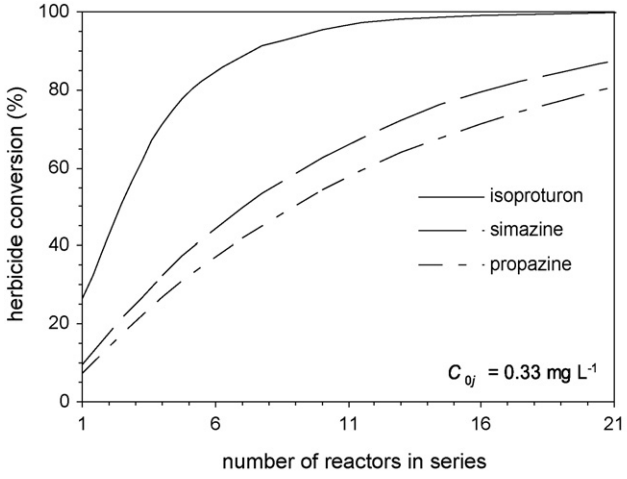

Fig. 5. Effect of number of reactors in series on conversions of a multicomponent herbicide solution ($C_{0j} = 0.33$ mg L^{-1} each). $Q^0 = 0.4$ L min^{-1}; $c_{cat} = 3$ kg m^{-3}; diffuse photon scattering ($p_b = 0.71$; $p_f = 0.11$; $p_s = 0.045$) [21]; other conditions from Table 4.

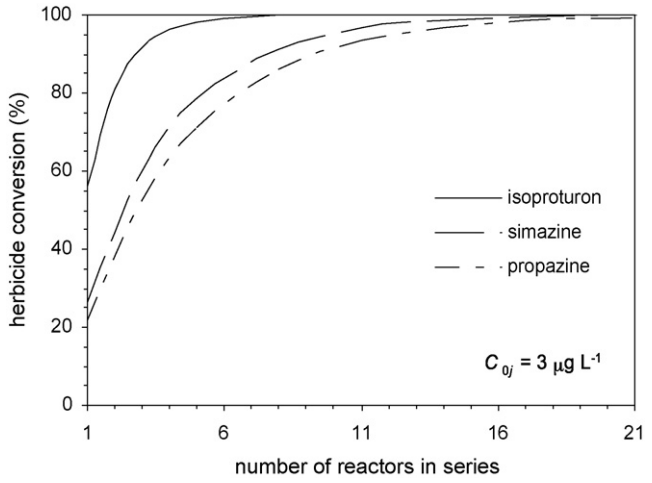

Fig. 6. Effect of number of reactors in series on conversions of a multi-component herbicide solution (C_{0j} = 3 μg L^{-1} each). Q^0 = 0.4 L min^{-1}; c_{cat} = 3 kg m^{-3}; diffuse photon scattering (p_b = 0.71; p_f = 0.11; p_s = 0.045) [21]; other conditions from Table 4.

the herbicide concentration in the feed stream to the series reactors, the Damkholer number increases, and in consequence herbicide conversions are expected to increase. Fig. 6 shows these simulations when the herbicide concentrations in the feed equal 3 μg L^{-1} each. Isoproturon is fully converted in 8 reactors and isoproturon and simazine in 20 reactors. Further decreases in the herbicide feed concentration from this level does not change the conversion profiles further, since the apparent rate constant in the herbicide rate laws remains practically constant. It should be noted that typical concentrations of herbicide in contaminated groundwater and or surface water are in the range from 0.1 μg L^{-1} to a few μg L^{-1}.

3.5. Scaling-up to plant scale

Water treatment by PCO in general should be applied to contaminated streams with low flowrates. Table 6 summarizes plant specifications and treatment costs for a plant-scale treatment facility. Operating costs are dominated by electricity costs. Catalyst and lamp replacement account for 20% of the total operating cost. For the plant described in Table 6 the total operating cost is 3.75 Euro m^{-3}. There is ample scope of reducing this cost further, by one-order of magnitude, by either using solar radiation [28] or by using PCO in combination with an oxidant and UVC radiation [23]. Therefore, we anticipate that the use of PCO for treatment of herbicides residues in water could be economically competitive against current treatment methods employing adsorption by granular activated carbon.

Table 6
Plant specifications and treatment cost to treat mixtures of isoproturon, simazine and propazine in water

Plant specifications	
Operating time	24 h day^{-1}
Flow rate	5.76 m^3 day^{-1}
Herbicides feed concentration	Up to 3 μg L^{-1}
Herbicides conversion	Each > 80%
Catalyst concentration (TiO_2 Degussa P25)	3 kg m^{-3}
Catalyst loss (@ 5% per day)	0.12 kg day^{-1}
Number of reactors (10 × 10 in series)	100
Reactors foot print	4 m^2
Volume of suspension in 100 reactors	0.8 m^3
Electrical energy for UV lamps	3.6 kWh
Electrical energy for pumps	3.6 kWh
Operating costs	
Electricity cost (@ 0.1 Euro kWh^{-1})	3 Euro m^{-3}
Lamp replacement cost (@ 6.5 Euro/lamp)	0.23 Euro m^{-3}
Catalyst replenishment cost (@ 25 Euro kg^{-1})	0.52 Euro m^{-3}

4. Conclusions

This work has shown the scale-up of laboratory kinetics rate data to plant scale to treat water contaminated with three common herbicides. The kinetics of the photocatalytic oxidation of the herbicides isoproturon, simazine and propazine in multicomponent systems were studied in a laboratory-scale annular photoreactor. It was successfully modeled by an approximation of the Langmuir-Hinshelwood rate equation, which included the effect of the intermediate products, using kinetic parameters determined in single-component experiments. Intrinsic kinetic parameters were determined by an accurate description of the reaction kinetics and the radiation field in the reactor. Herbicide conversions in an optimized configuration of a pilot-scale falling film photoreactor were estimated by a mathematical model of the photoreactor and the implementation of the reaction kinetics established in the laboratory-scale reactor. The conversion results, as a function of the number of reactor modules connected in series, were used to predict plant specification and operating costs. This analysis is essential at the design stage of photocatalytic water treatment plants.

The method presented allows the derivation of reaction rate laws and reaction kinetic constants which are independent of the radiation field in the reactor and therefore more universally applicable to the design and scale-up of photocatalytic reactors compared to semi-empirical rate laws based on the incident flux or on the overall radiation absorbed in the photoreactor.

Acknowledgements

The authors are grateful to NATO (Grant SfP-977986) and the EU Socrates-Erasmus Programme for the financial support to produce this work.

References

[1] F. Worrall, T. Besien, D.W. Kolpin, Sci. Total Environ. 299 (2002) 131.
[2] K. Bester, A Pesticide Inventory in German Surface and Coastal Waters, WWF report, WWF North-East Atlantic Programme, Germany, 1998.
[3] R.J. Gilliom, J.E. Barbash, D.W. Kolpin, S.J. Larson, Environ. Sci. Technol. 33 (1999) 164A.
[4] D. Hamilton, S. Crossley, Pesticide Residues in Food and Drinking Water—Human Exposure and Risks, John Wiley & Sons, 2004.
[5] I.K. Kostantinuou, T.A. Albanis, App. Catal. B: Environ. 42 (2003) 319.
[6] J.-M. Herrmann, C. Guillard, C.R. Acad. Sci. Paris, Ser. IIc, Chimie/Chemistry 3 (2000) 417.

[7] S. Malato, J. Blanco, J. Caceres, A.R. Fernandez-Alba, A. Aguera, A. Rodriguez, Catal. Today 76 (2002) 209.
[8] M.R. Hoffmann, S.T. Martin, W. Choi, D.W. Bahnemann, Chem. Rev. 95 (1995) 69.
[9] C.S. Turchi, D.F. Ollis, J. Catal. 172 (2000) 178.
[10] S. Parra, J. Olivero, C. Pulgarin, Appl. Catal. B: Environ. 36 (2002) 75.
[11] A. Gora, B. Toepfer, V. Puddu, G. Li Puma, Appl. Catal. B: Environ. 65 (2006) 1.
[12] B. Toepfer, A. Gora, G. Li Puma, Appl. Catal. B: Environ. 68 (2006) 171.
[13] A.E. Cassano, O.M. Alfano, Catal. Today 58 (2000) 167.
[14] O.M. Alfano, A.E. Cassano, J. Catal. 172 (1997) 370.
[15] C.S. Turchi, D.F. Ollis, J. Catal. 122 (1990) 178.
[16] O.M. Alfano, M.I. Cabrera, A.E. Cassano, J. Catal. 172 (1997) 370.
[17] D.F. Ollis, in: E. Pelizzetti, M. Schiavello (Eds.), Photochemical Conversion and Storage of Solar Energy, Kluwer Academic Publishers, Dordrecht, 1991, pp. 593–622.
[18] J.-M. Herrmann, Top. Catal. 34 (2005) 49.
[19] G. Li Puma, J.N. Khor, A. Brucato, Environ. Sci. Technol. 38 (2004) 3737.
[20] G. Li Puma, A. Brucato, Catal. Today 122 (2007) 78.
[21] A. Brucato, A.E. Cassano, F. Grisafi, G. Montante, L. Rizzati, G. Vella, AIChE J. 52 (2006) 3882.
[22] G. Li Puma, P.L. Yue, Ind. Eng. Chem. Res. 38 (1999) 3246.
[23] G. Li Puma, P.L. Yue, Environ. Sci. Technol. 33 (1999) 3210.
[24] Philips Lighting Catalogue, Special Lighting, Blacklight Blue Fluorescent, www.philips.com.
[25] G. Li Puma, Environ. Sci. Technol. 37 (2003) 5783.
[26] R.B. Bird, W.E. Stewart, E.N. Lightfoot, Transport Phenomena, second ed., John Wiley & Sons, New York, 2002.
[27] S.M. Jacob, J.S. Dranoff, Chem. Eng. Prog. Symp. Ser. 62 (1966) 47.
[28] S. Malato, J. Blanco, C. Richter, M.I. Maldonado, Appl. Catal. B: Environ. 25 (2000) 31.